Compressive Strength of Solid Clay Brickwork: Calibration of Experimental Tests

by

C BILELLO[1], A BRENCICH[2], M DI PAOLA[1] and E STERPI[2]
[1] *Department of Structural and Geotechnical Engineering, University of Palermo*
[2] *Department of Structural and Geotechnical Engineering, University of Genoa*

ABSTRACT
The assessment procedures for masonry structures require some mechanical parameters to be defined for masonry, at least the compressive strength. Several theoretical approaches, based on the characteristics of the constituents, i.e. bricks and mortar, have been developed but their application to existing masonry turns out to be rather difficult. Therefore, experimental approaches give a fundamental contribution to the identification of the mechanical parameters provided that proper calibration allows a reliable estimation of the experimental error. In this paper, the calibration of compressive tests on large diameter cylinders, drilled from brickwork and loaded on the lateral surfaces, is discussed on the bases of both experimental and theoretical issues. This technique is shown to reproduce the brickwork collapse mechanism, giving reliable estimates of the masonry compressive strength.

1. INTRODUCTION

A large number of old masonry structures, such as arch bridges, tunnels, historical and ordinary buildings, are still in service facing either increased loads or material degradation. Due to their fundamental role in transportation systems and in European cities, the assessment of their safety level with respect to modern standards has become a primary need. Whatever the mechanical model for the structure and the material constitutive model, the assessment procedure requires some mechanical parameters to be identified, at least the compressive strength f_c and, sometimes, also the elastic parameters (E and ν) and others. The available experimental and theoretical approaches present both advantages and uncertainties, so that the assessment procedures require both the approaches to be used; nevertheless, the estimate of the global error introduced into the structural models, and therefore of the reliability of the final results, remains quite difficult.

The experimental approach to existing masonry relies on Non-Destructive or Minimally-Destructive Tests (NDT or MDT). These face some conceptual deficiencies for some techniques, a limited data base for the test calibration and large errors due to specific technical problems for other techniques. For example, the core of small diameter drillings, i.e. 70-90mm, does not reproduce the brickwork bond; if the cores are loaded on the bases, following well established techniques for concrete, the loading direction is different from that of the real structure and the result, according to the position of the mortar joint inside the core, may dramatically overestimate or seriously underestimate the actual compressive strength of the masonry. Flat jacks [1], as a second example, require highly skilled workmanship and a precise, and expensive testing procedure to provide reliable results such that, in practice, large differences may occur with this technique. Other NDT approaches proposed, such as radar and sonic testing [2-4] due to the high intrinsic inhomogeneity of masonry, still need a detailed calibration and do not seem to be capable of providing quantitative estimates of the brickwork mechanical parameters, at least, at this level of research.

Deformation and failure theories, on the other hand, have been developed since the late sixties with the aim of defining constitutive models and failure criteria based on the mechanical properties of the brickwork constituents, i.e. bricks and mortar [5-12]. The basic assumption looks at masonry as an unlimited layered continuum in plane strain conditions, thus assuming uniform stress distributions in the materials and neglecting the boundary effects. Due to the elastic mismatch between bricks and mortar, this assumption implies that brickwork collapse is attained when a tensile limit condition is met in the brick, while the 3D compressive stress state in the mortar makes this component of minor importance in the global response. Due to the stress concentrations induced by masonry intrinsic inhomogeneity, and to the difficulty in the mechanical identification of bricks and mortar, the theoretical approaches do not give satisfactory estimates of the experimental data either of the measured compressive strength or of the elastic modulus.

In this work an experimental procedure for solid clay brickwork, by far the most common type of masonry, is discussed and partially calibrated. Compressive tests on large diameter cylinders (ϕ = 150mm) loaded on the lateral surface have been proposed by UIC [13]. The advantages of this test are: a) the brickwork bond is represented in the specimen; b) the load direction is normal to the horizontal mortar joint as in the actual brickwork. The calibration of the test outlines that: i) the collapse mechanism of the specimen is similar to the collapse mechanism of brickwork; ii) the effect of local concentrations of stresses, due to the testing setup, on the measured compressive strength seems to be of minor importance; iii) a calibrated formula for the compressive strength (and elastic modulus) to be used for practical applications and an estimate of the inherent error can be deduced.

2. TESTING PROCEDURES

2.1 The experimental approach

The UIC 778-3R guidelines [13] require a ϕ = 150mm diameter cylinder to be drilled so as to reproduce the basic brickwork bond, Figure 1. The specimen is loaded on the lateral surface, i.e. in the same way brickwork is loaded in the original structure, recording both the vertical and horizontal displacements. The compressive strength f_c of brickwork is simply assumed as the ratio between the collapse load F_{coll} and the horizontal cross section $\phi\, l$, Figure 2, being l the cylinder length; the characteristic value of the compressive strength is assumed as 1.1 times the minimum value. The secant elastic modulus is calculated referring to a reduced section $0.75\phi\, l$ and to loads at 1/10th ($F^{0.1}$) and 1/2 ($F^{0.5}$) of the limit load:

$$f_c = F_{coll}/\phi\, l, \qquad \text{(1.a, b)}$$

$$\varepsilon_h = u_h/\phi, \qquad \text{(2.a, b)}$$

$$\Delta\varepsilon_h^{0.1\text{-}0.5} = u_h^{0.5} - u_h^{0.1}/\phi, \qquad \text{(3.a, b)}$$

$$E = 4(F^{0.5} - F^{0.1}) / 3(u_v^{0.5} - u_v^{0.1})l,$$
$$v = u_h^{0.5} - u_h^{0.1} / u_v^{0.5} - u_v^{0.1}, \quad (4.a, b)$$

being ε_v and ε_h the vertical and horizontal strains and u_v and u_h the related displacements.

The testing set-up is presented in Figure 2; minor details are omitted for simplicity [14]. The load measuring device is a C5 class *HBM-RTN* load cell with a 0.01% precision and is located in-between the upper plate and the testing machine. The upper and lower plates are connected to the testing frame through cylindrical hinges that allow the load line to be precisely identified. The relative displacements are measured by means of LVDTs with a 0.001mm precision. The displacement of the upper plate is measured at the two ends of the specimen (LVDTs n. 1 and 2), while the lateral ones are recorded at the centre of the cylinder (LVDTs n. 3 and 4), so that u_v, Equation (2) and (3), is directly the sum of devices 3 and 4.

The moving end of the machine, and the whole load process, is displacement controlled, the load being measured by the load cell. The load cell can be considered as a spring with high stiffness; up to the limit load this does not affect the results at all; it significantly alters the measurements only far after the material collapse at a point when the softening curve has already lost any mechanical meaning. A 2mm thick lead sheet between the specimen and the loading plates was used to smooth the lateral surface of the cylinder.

2.2 Testing program and research aims

The calibration of the test may be obtained by comparison of the measured data with the compressive strength of the brickwork. The latter is substantially unknown and, in the frame of a test calibration, is obtained through concentric load tests on prisms of the same type of masonry (identical materials, workmanship, hygrometric and curing conditions etc.). For this reason, not only was a large number of tests performed in order to provide a reasonably large data base, but also specimens were produced in pairs at the same time, one for drilling the cylinder and the other for direct testing. For these reasons, tests are compared two-by-two: test on cylinder vs. direct compression test on concentrically loaded prisms, Figure 3.

Three types of solid clay brickwork were used: 1) Brickwork 1: modern solid bricks (Brick 1) with a cement-lime mortar (Mortar 1); 2) Brickwork 2: modern solid bricks (Brick 1) with a white cement-lime mortar (Mortar 2); 3) Brickwork 3: engineering bricks (Brick 2) with a cement-lime mortar (Mortar 3). Table 1 shows the data for the materials deduced according to [15-17]. Mortar 1 (cement-lime) and Mortar 2 (white cement – lime) are different commercial Italian products for which the producer did not provide the exact proportions, while Mortar 3 is a self produced 1:1:5 mortar with water/cement volume ratio = 0.7. In this way the calibration procedure may rely on previous data on an historic masonry [14] and on other three substantially different brickwork types.

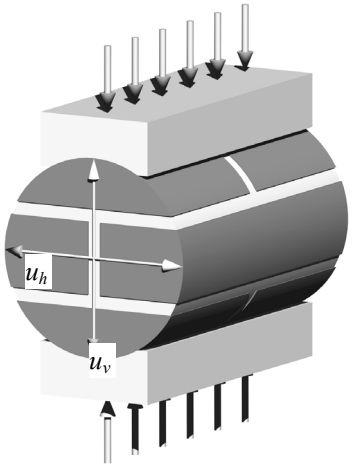

Figure 1 Test arrangement

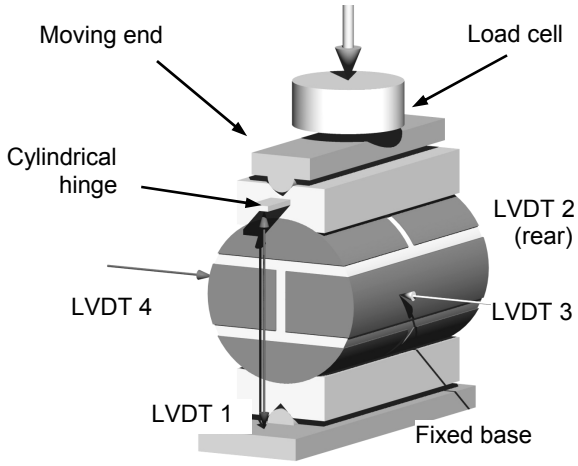

Figure 2 Detail of test arrangement

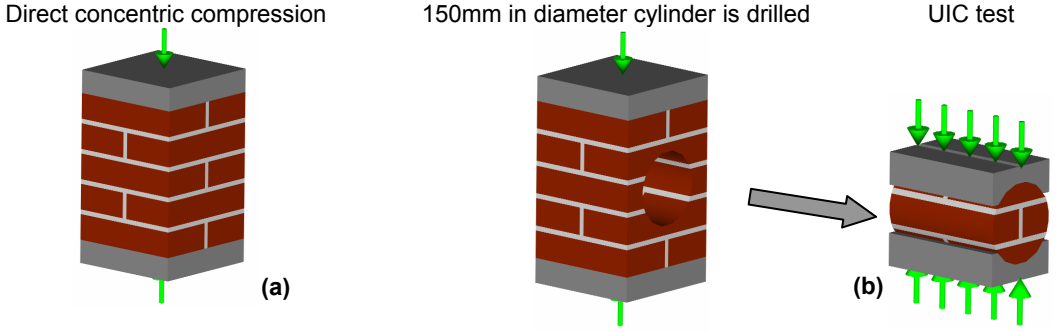

Figure 3 Identical specimens for: (a) direct concentric compression; (b) UIC (1995) tests

Table 1
Mechanical characteristics of bricks and mortars

		Av. value [N/mm^2]	n. of samples	C.o.V.	Char. Value[1] [N/mm^2]	Char. / Average
Brick 1*	Compressive strength – direct	20.2	20	17%	13.6	0.67
	Tensile strength – TPB	5.0	10	6.5%	4.30	0.86
	Elastic modulus	15930	20	32%	5930	0.38
Brick 2+	Compressive strength – direct	32.5	12	17%	26.0	0.80
	Tensile strength – TPB	0.8	6	10%	0.7	0.84
	Elastic modulus	26200	12	30%	13070	0.50
Mortar 1*	Compressive strength – direct	11.9	25	3%	11.5	0.97
	Tensile strength – TPB	3.8	13	8%	3.5	0.92
	Elastic modulus	1520	25	3%	2440	0.97
Mortar 2*	Compressive strength – direct	8.9	32	5%	8.5	0.96
	Tensile strength – TPB	3.3	16	4%	3.2	0.97
	Elastic modulus	1300	32	17%	1080	0.83
Mortar 3+	Compressive strength – direct	<6.9>	13	10.6%	5.7	0.83
	Tensile strength – TPB	<1.4>	6	6.4%	1.25	0.89
	Elastic modulus	<5.635>	4	3.6%	5.298	0.94

* Genoa +Palermo [1] Gaussian distribution assumed

3. TEST RESULTS

Figures 4 to 7 show the stress-strain curves and the collapse mechanisms of the specimens tested. Table 2 summarizes the experimental data (Prism 3 for Brickwork 1 and Cylinder 3 for Brickwork 3 are missing because of technical problems during the tests). Stresses are calculated as suggested by UIC, i.e. dividing the peak load by the whole horizontal section ϕl.

Figure 4 show that the overall response of prisms and cylinders have similarities and differences: i) the peak load and the (elastic) initial stiffness are rather different but the ratio between the cylindrical tests and the prism data seems to be fairly constant, Table 2; ii) in a similar way, also the elastic (initial) stiffness seems to be different but with a constant ratio; iii) the post peak response seems to be quite similar for both prisms and cylinders; iv) cylinders exhibit a longer softening phase than the prisms as a consequence of the confining effect of the loading plates. Figures 5 and 7 show that the collapse mechanism of Brickwork 1 and 2 is almost the same for both prisms and cylinders; Figure 6 shows that when high strength bricks (engineering bricks) are used (Brickwork 3), the cylinder collapse mechanism is different from that of the prisms: the brick/mortar interface collapses and the lateral parts of the cylinder detach from the specimen before cracking is activated in the central joint, while this does not happen in the prisms of the same masonry. When strong bricks are coupled with (relatively) weak mortar, the cylinders seem to collapse because of the stress concentration induced by the loading plates. The latter conclusion needs a wider data base to rely on before general conclusions are derived.

The tests show rather similar post-peak descending branches of prisms and cylinders and significant inelastic strains, more pronounced for cylinders due to the confining effect of the loading plates. Figure 5(a) shows the typical collapse mechanism at approximately 80% of the peak load when the central vertical mortar joint cracks along its whole length, outlining that inelastic strains have already been developed. Figure 5(b) displays the collapse mechanism at collapse. Figures 5(c)-(e) show the final stage of the specimen: i) a crack is found in the vertical joint, at the mortar/brick interface or inside the joint; ii) the lateral parts of the specimen are detached, the phenomenon being induced by the ends of the loading plates (Figure 5(b)). Figure 6 shows a different mechanism for type 3 brickwork.

4. NUMERICAL APPROACH: FEM MODELS

FEM models may help in understanding the collapse mechanism of the cylinders. The numerical approach usually fails to reproduce the whole collapse mechanism because of numerical instabilities that arise when diffused cracking is spread throughout the brickwork. Experimental tests show that the pre-peak and post-peak phases exhibit large cracking as a result of the non linear load-displacement response. Since the simulation of these phases is quite difficult for FEM models, a numerical approach can be used to understand better the activation of cracking and the first steps of its evolution. In the following, the main results of FEM analysis [14] for brickwork similar to the one tested in this work are briefly summarized with the aim of outlining the evolution of cracking at the beginning of the inelastic phase, as shown in Figure 5(a).

Figure 8 shows the load-displacement curve of the FEM model. On the right-hand side the load-vertical displacement curve shows that, in spite of a rather diffused cracking, the specimen does not exhibit a macroscopic non linear behaviour, whilst the lateral displacement, left-hand side of Figure 8, shows a curve with two distinct parts: at step 4 the stiffness suddenly decreases as cracking is activated in the vertical joint (Figure 5(b)): after step 4 the stiffness remains approximately constant at the reduced value while cracks propagate inside the bricks (Figure 9): the gradual activation of the central core of brickwork that had been already detected during the tests is noticeable.

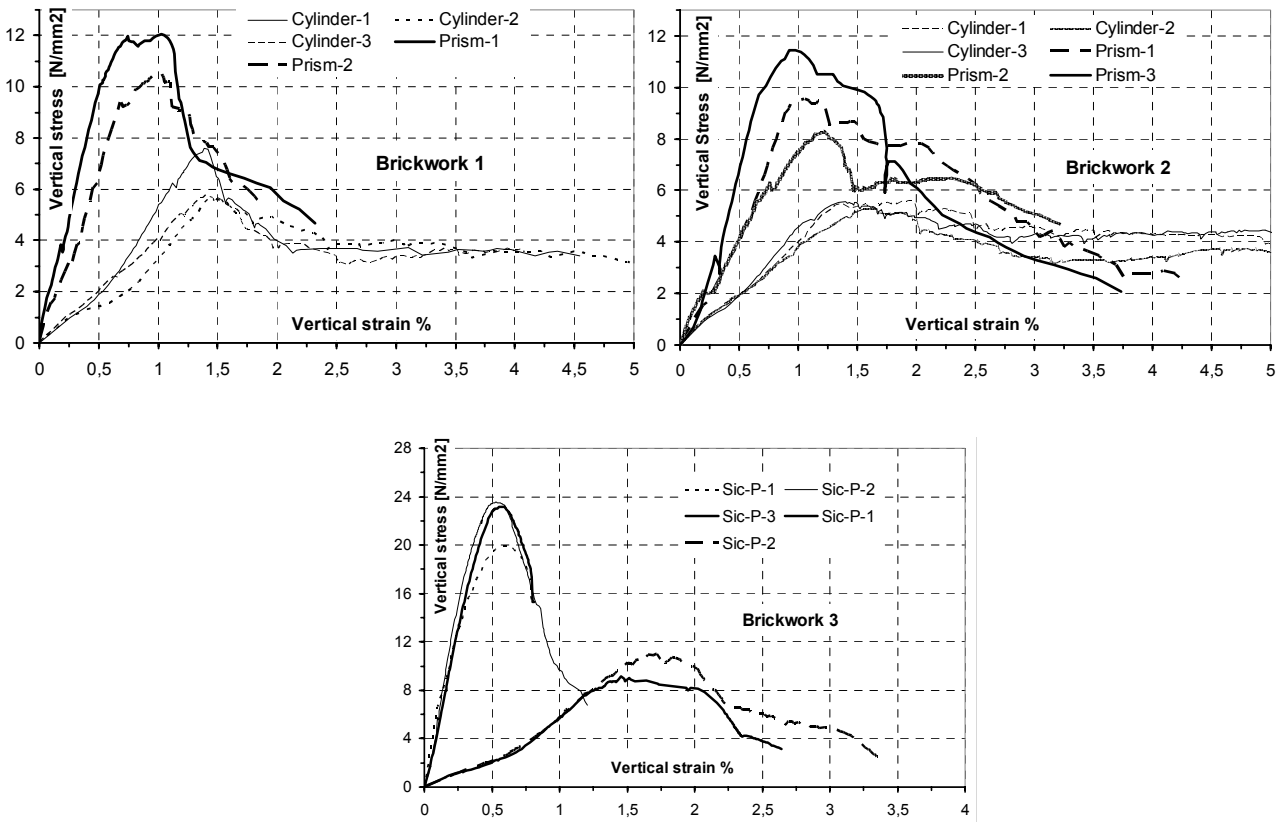

Figure 4 Stress-strain curves for brickwork: (a) type 1; (b) type 2; (c) type 3

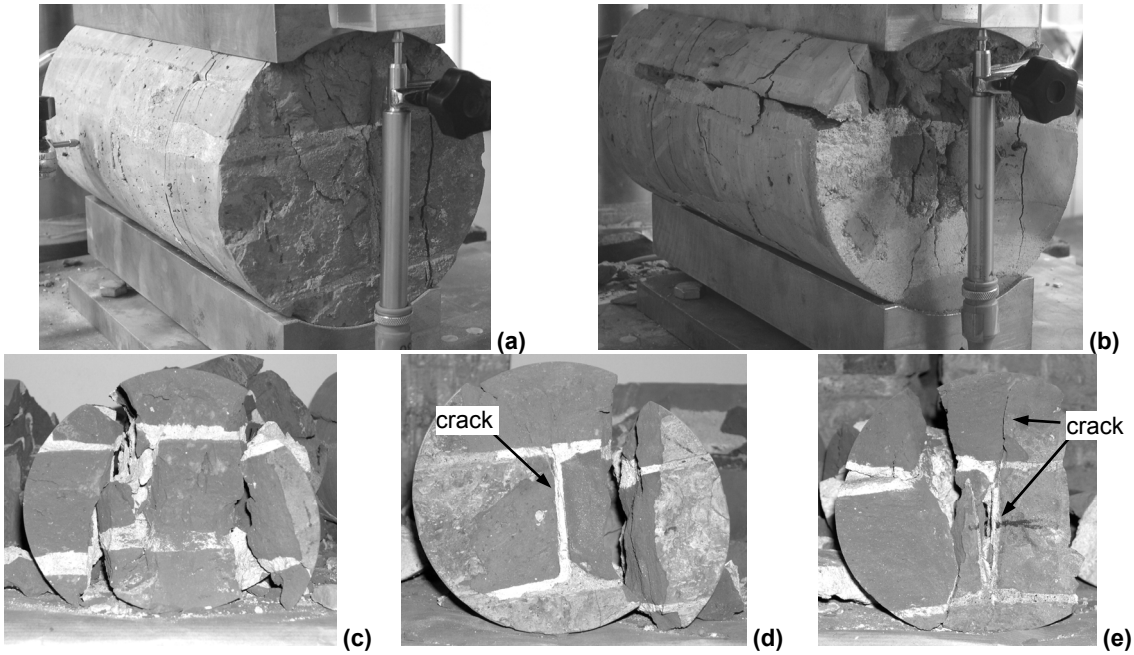

Figure 5 BRICKWORK 1 and 2: typical crack pattern at: (a) 80% of the maximum load; (b) end of the test; (c), (d) and (e) typical collapse mechanisms: opening of the vertical joint and splitting of the lateral part of the cylinder (after peak load)

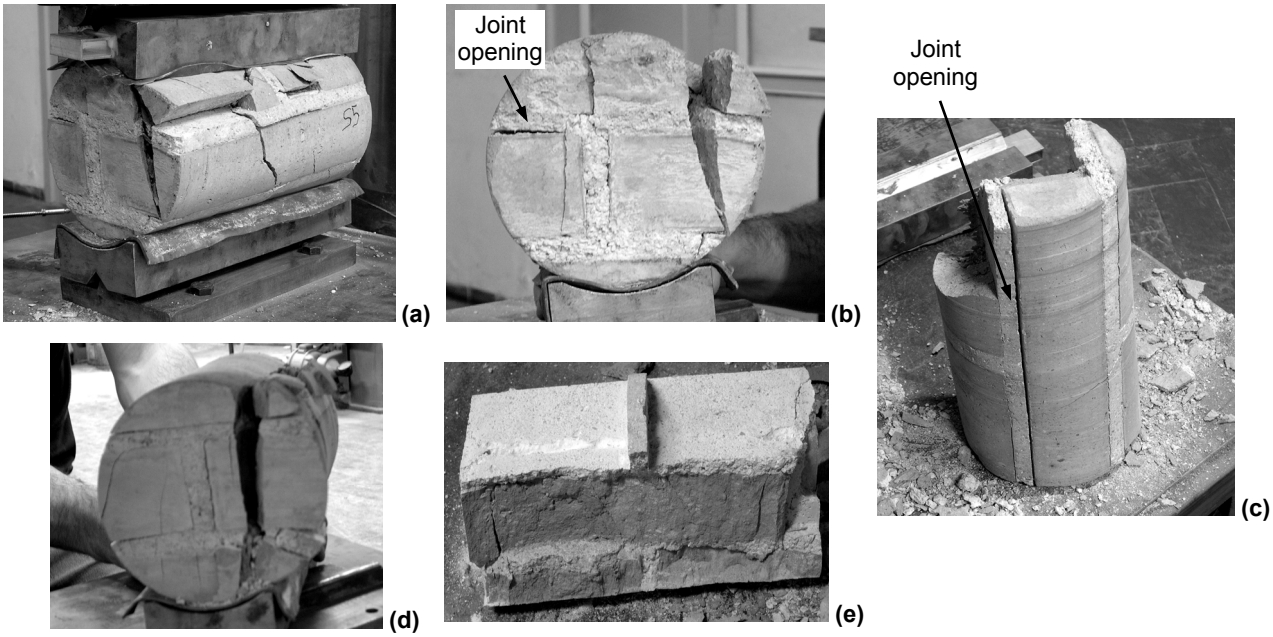

Figure 6 BRICKWORK 3: typical crack pattern at the maximum load. Cylinder 1: (a) the lateral parts detach and (b) the brick/mortar interface collapses before the collapse mechanism is activated; (c) clear detachment of the joint. Cylinder 2: (d) the same collapse mechanism observed for Cylinder 1; (e) detachment also of the horizontal joints

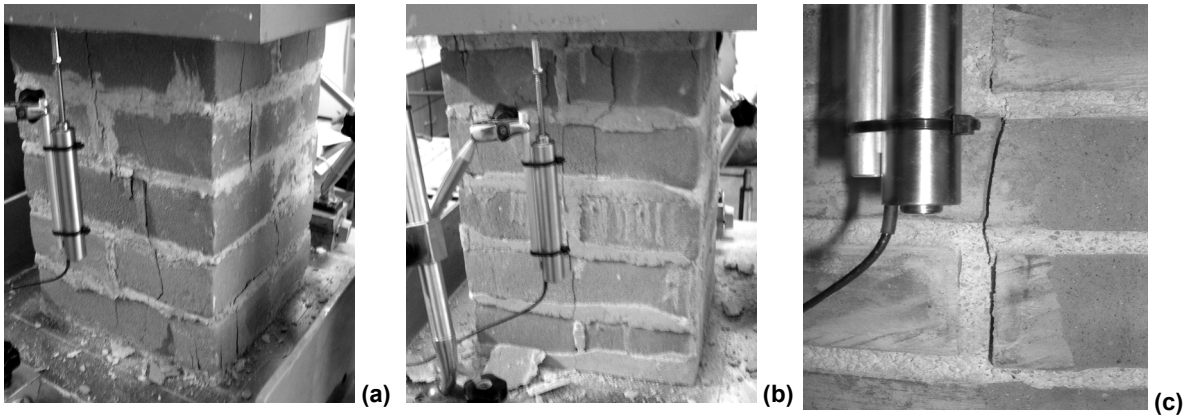

Figure 7 Cracking of masonry prisms at approx. 80% of the peak load: (a) and (b) lateral views; (c) detail

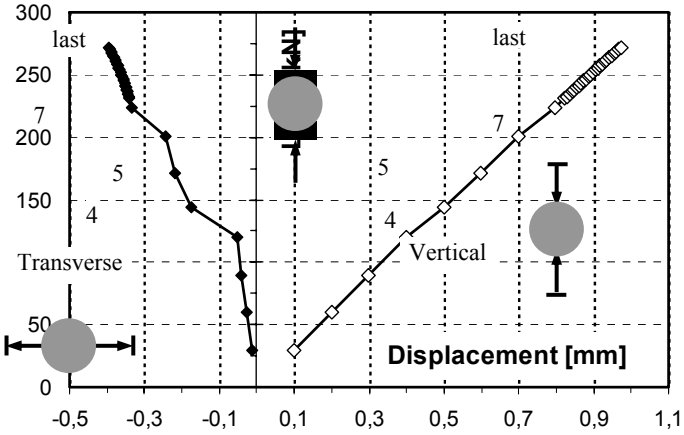

Figure 8 Load-Displacement (vertical and horizontal) response of the numerical model

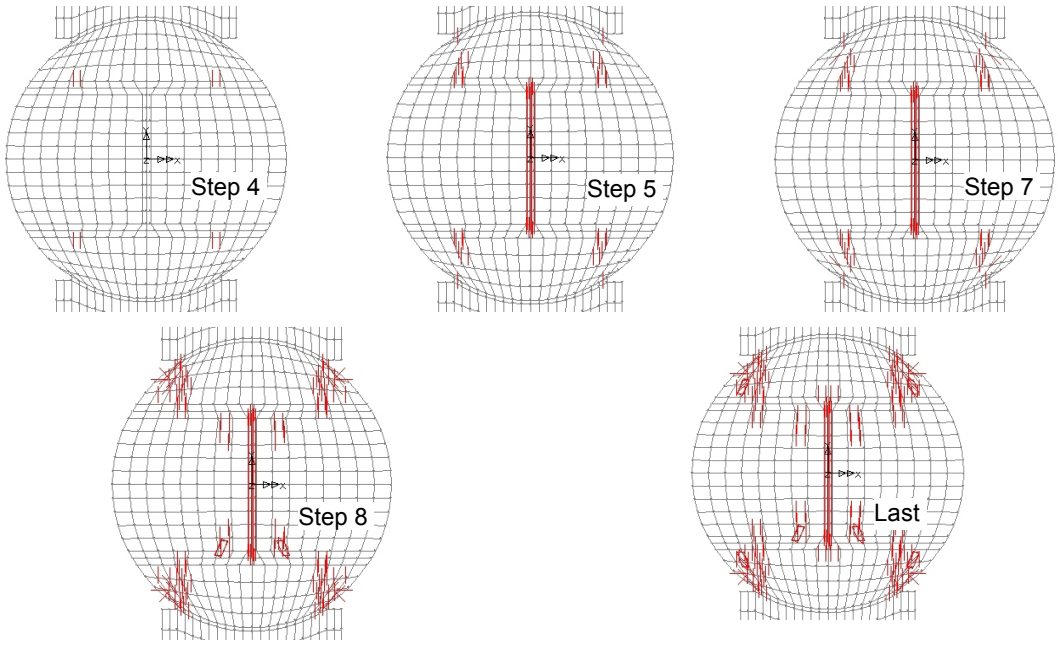

Figure 9 Crack pattern evolution during the load process (see Figure 5)

Table 2
Summary of the experimental data

BRICKWORK 1 - Brick 1 + Mortar 1						
	Prism 1	**Cylinder 1**	**Prism 2**	**Cylinder 2**	**Prism 3**	**Cylinder 3**
f_c [N/mm^2]	12.1	7.6	10.6	5.7	/	5.8
E [N/mm^2]	20550	6820	15560	5140	/	4070
f_c prism/cylinder	1.6		1.9		/	
E prism/cylinder	3.0		2.8		/	
BRICKWORK 2 - Brick 1 + Mortar 2						
	Prism 1	**Cylinder 1**	**Prism 2**	**Cylinder 2**	**Prism 3**	**Cylinder 3**
f_c [N/mm^2]	9.6	5.6	8.2	5.3	11.5	5.6
E [N/mm^2]	12900	4000	9500	3400	19300	5080
f_c prism/cylinder	1.7		1.6		2.1	
E prism/cylinder	3.2		2.8		3.7	
BRICKWORK 3 - Brick 2 + Mortar 3						
	Prism 1	**Cylinder 1**	**Prism 2**	**Cylinder 2**	**Prism 3**	**Cylinder 3**
f_c [N/mm^2]	20.0	9.1	23.6	11.0	23.2	/
E [N/mm^2]	29000	9400	23560	7000	31080	/
f_c prism/cylinder	2.2		2.1		/	
E prism/cylinder	3.1		3.4		/	

The distribution of the vertical and horizontal stresses at approximately 80% of the peak load is shown in Figure 10. The vertical stresses (Figure 10(a)) are not distributed through the whole cross section but are concentrated in a sand-glass shaped central core containing as much as 60% of the whole cross section. The stress distribution is not uniform being affected by the cracking of the vertical joint. Figure 10(b) shows strong concentrations of horizontal stress in the upper and lower bricks close to the edges of the loading plates. This explains the observed crack patterns and the detachment of the lateral parts of the cylinders (Figures 5(c)-(e) and 9).

The FEM model, although not capable of reproducing the entire loading process up to collapse, helps in understanding the onset of cracking in the specimen. Figure 7 shows the crack pattern at approximately 80% of the peak load for the tested prisms, where cracking clearly originates from the central mortar joint. Some ongoing numerical analysis [12] suggests that this is caused by a concentration of tensile stresses in the brick, in the part close to the vertical joint, due to the brick/mortar elastic mismatch. The comparison of the crack pattern of Figures 5, 6 and 7 with the results of the numerical analysis shows that the brickwork collapse mechanism is reproduced by the large diameter cores but for the stress concentrations due to the loading plates (Figure 10(b)). For these reasons, a calibration of the test can be performed providing reliable estimates of the actual brickwork compressive strength.

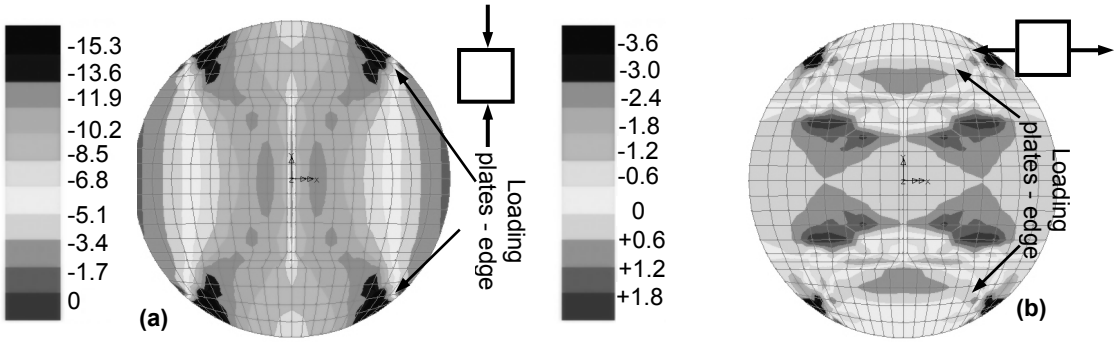

Figure 10 (a) Vertical and (b) horizontal stresses [MPa] at 80% of the peak load

5. COMPARISON AND DISCUSSION

The compression tests on the cylinders show a collapse mechanism similar to that of solid clay brickwork prisms, both in the crack evolution and in the stress/strain response; the post peak phase is much more ductile (see [18] for a definition of brickwork ductility) than that which is found for brickwork prisms due to the confinement of the loading plates. Nevertheless, the ratio between the compressive strength and the elastic modulus measured on the cylinders and on prisms, the latter representing the reference masonry, is reasonably constant. Due to the large differences in the post peak phase, no information on masonry ductility can be deduced from the cylinder tests.

On the bases of the results summarized in Table 2, a first calibration of the test can be given by the formulae:

$$f_c^{prism} \cong 1.8\, f_c^{cyl}, \text{ and } E^{prism} \cong 3E^{cyl} \qquad (5a, b)$$

which can be considered valid for bricks with compressive strength not larger than 25-30N/mm^2. Similar conclusions have already been derived by some of the authors in a previous research [14]. For higher compressive strengths, the calibration coefficients seems to be higher (Table 2) but a general conclusion cannot be derived at this stage of the research.

The C.o.V. of the compressive strength is approximately 30% for both the cylinders and the prisms (7% for the cylinder and 24% for the prism tests if the anomalous prism n. 1 of Table 2 is not considered) which is fairly typical for small brickwork assemblages [19-20]. Assuming a Gaussian distribution, the characteristic values for the compressive strength is:

$$f_{ck}^{prism} \cong 1.3 \langle f_c^{cyl} \rangle, \qquad (6)$$

where $\langle f_c^{cyl} \rangle$ is the average value of the cylinder tests. It seems that there is no reason for referring to the minimum experimental value, Equation (1b); if large dispersion of experimental data is found, the coefficient of Equation (6) can be modified according to the standard semi-probabilistic approach to material strength on the basis of the number of tests performed.

The C.o.V. of the elastic modulus is approx. 57%; such a high value shows that no reliable information can be deduced from the large cylinder test on material deformability. Similar results had already been obtained by the authors in a previous calibration campaign (BRENCICH et al., 2004). This result is not unexpected: the elastic modulus is a unique parameter for the whole structure, in other words it is a global parameter, an average property of average brickwork, while experimental tests are always local measurements. Apart from the error in the specific technique, any test is affected by the inhomogeneity of the material; the smaller the specimen the larger the effect of these in homogeneities on he experimental outcome. In the specific case of brickwork cylinders, the specimen represents a very small part of the material, only partially reproducing the brickwork bond. In the experimental set-up, for example, the lead sheets between the loading plates and the specimen and geometric irregularities of the cylinder are only two of the reasons explaining the large variability in the elastic modulus measurements. For these reasons, Equation (5b) should be applied very carefully for the identification of the Young's modulus, considering that the test reliability is very low. A better way for the identification of the elastic modulus is that of dynamic tests on the original structure, which are tests on the whole structure for the identification of a global mechanical parameter [21].

REFERENCES

1. ASTM Standard C1196-91. *In situ compressive stress within solid unit masonry estimated using flatjack measurements*.
2. COLLA, C, MCCANN, D M and FORDE, M C. Radar testing of masonry arch bridges with soil backfill, Proc. *II Int. Arch Br. Conf.*, 253-261, Balkema, Rotterdam, 1998.
3. BENSALEM, A, ALI-AHMED, H, FAIRFIELD, C A and SIBBALD, A. NDT as a tool for detection of gradual safety factor deterioration in loaded arches, Proc. *II Int. Arch Br. Conf.*, 271-277, Balkema, Rotterdam, 1998.
4. VALLE, S, ZANZI, L, BINDA, L, SAISI, A and LENZI, G. Tomography for NDT applied to masonry structures : Sonic and/or EM methods, Proc. *II Int. Arch Br. Conf.*, 243-252, Balkema, Rotterdam, 1998.
5. HILSDORF, H K. Investigation into the failure mechanism of brick masonry under axial compression, in Designing, Eng.ng & Construction with Masonry Products, F.B. Johnson ed., Gulf Publishing, Houston, Texas, 1969.
6. FRANCIS, A J, HORMAN, C B and JERREMS, L E. The effect of joint thickness and other factors on the compressive strength of brickwork, Proc. 2nd I. B. MA. C., Stoke on Kent, 1971.
7. KHOO, C L and HENDRY A W. A failure criteria for brickwork in axial compression, Proc. 3rd I.B.Ma.C., Essen, 141-145, 1973.
8. ATKINSON, R H and NOLAND, J L. A proposed failure theory for brick masonry in compression, Proc. of the 3rd Can. Mas. Symp., Edmonton, 1983.
9. SHRIVE N G. 'A fundamental approach to the fracture of masonry', Proc. 3rd Can. Mas. Symp., Edmonton, 4/1-4/16, 1983.
10. BIOLZI, L. Evaluation of compressive strength of masonry walls by limit analysis, *J. of Str. Eng.ng*, **114**, 2179-2189, 1988.
11. MILANI, G. Homogenization techniques for in and out of plane loaded masonry walls, *Ph.D. Thesis*, University of Ferrara, 2005.
12. CORRADI, C. *Theoretical and experimental analysis of the strength of eccentrically loaded brickwork* (in Italian), Ph.D. Thesis, Dept. of Str. and Geotech. Eng.ng, Univ. of Genoa, 2006.
13. UIC – International Union of Railways: UIC code 778-3R, 1995, *Recommendations for the assessment of the load carrying capacity of the existing masonry and mass-concrete arch bridges*.
14. BRENCICH, A, CORRADI, C and STERPI, E. Experimental approaches to the compressive response of solid clay brickwork, *13th IBMaC.*, 4-7 July, Amsterdam, 2004.
15. prEN 771-1. 1999. *Specification for masonry units-Part1: Clay masonry units*, September 1999.
16. prEN 772-1. 1999. *Methods of test for masonry units - Part1: Determination of compressive strength*, Febr. 1999.
17. prEN 1052-1. *Methods of test for masonry -Part1: Determination of compressive strength*, Sept. 1998.
18. BRENCICH, A and GAMBAROTTA, L. Mechanical response of solid clay brickwork under eccentric loading. Part I: Unreinforced Masonry, *Mat. and Str. (RILEM)*, **38**, 257-266, 2005.
19. ELLINGWOOD, B and TALLIN, A. Limit states criteria for masonry construction, *J. of Str. Eng.ng*, **111**, 108-122, 1985.
20. DYMIOTIS, C and GUTLEDERER, B M. Allowing for uncertainties in the modelling of masonry compressive strength. *Constr. and Build. Mat.*, **16**, 443-452, 2002.
21. BRENCICH, A and SABIA, D. (to appear). Experimental testing and structural models for a multi-span masonry bridge: the *Tanaro Bridge*. To appear on *J. of Bridge Eng.ng, ASCE*.